Hindawi
International Journal of Rotating Machinery
Volume 2023, Article ID 7622545, 11 pages
https://doi.org/10.1155/2023/7622545

Research Article

Research on Elastic Composite Cylindrical Roller Bearing Contact Fatigue Based on the Subsurface Stress

Wen Yang,[1] **Qishui Yao**,[2] **Jianghong Yu**,[2] **Yunxin Kuang**,[1] **and Jianfeng Huang**[1]

[1]*School of Intelligent Manufacturing, Hunan Railway Professional Technology College, Zhuzhou 412001, China*
[2]*School of Mechanical Engineering, Hunan University of Technology, Zhuzhou 412007, China*

Correspondence should be addressed to Qishui Yao; yaoqishui@126.com

Received 14 December 2022; Revised 1 April 2023; Accepted 27 April 2023; Published 17 May 2023

Academic Editor: Paramvir Singh

In order to study the elastic contact fatigue problems of composite cylindrical roller bearing, through the three stages of contact fatigue crack initiation, propagation, and ablating of cylindrical roller bearing theoretically analyzed, the subsurface stress is one of the factors of contact fatigue damage. By finite element method and theoretical analytic method with solid cylindrical roller bearing contact surface, the size and distribution of shear stress are analyzed, and comparing the calculation results of two methods, the comparison results show that the finite element method to calculate the bearing contact problem is scientific and reasonable. Through the finite element method of cylindrical roller bearing and elastic composite cylindrical roller bearing subsurface shear stress and equivalent stress on the surface of numerical analysis, the calculation results show that the subsurface stress value of elastic composite cylindrical roller bearings was 31.65% smaller than that of ordinary cylindrical roller bearings, and the distribution of the maximum subsurface stress value of elastic composite cylindrical roller bearings was shallower than that of cylindrical roller bearings. The elastic composite cylindrical roller bearings have significant advantages over cylindrical roller bearings in terms of subsurface stress and have stronger resistance to contact fatigue damage. The finite element method is used to analyze the subsurface stress of elastic composite cylindrical roller bearings with different filling degrees. The results show that the subsurface shear stress and equivalent stress values of elastic composite cylindrical roller bearings with filling degrees of 55% to 65% are maintained at a relatively low level, and the depth of the maximum stress is minimal, which is basically distributed on the surface of the rolling body. The magnitude and distribution of subsurface stresses in elastic composite cylindrical roller bearings provide a reference for more reasonable structural design.

1. Introduction

As a key component of rotating machinery, cylindrical roller bearing is also the main fault source of rotating machinery. It is generally believed that the fatigue with the number of cycles higher than 10^7 is called ultrahigh cycle fatigue, while the cylindrical roller bearing belongs to ultrahigh cycle fatigue. Under the action of complex alternating stress, the main failure form of cylindrical roller bearing is rolling contact fatigue. Fatigue crack is one of the manifestations of contact fatigue. The formation and growth of cracks are mainly affected by contact stress, and often, subsurface stress is the main source of crack formation and growth.

The contact fatigue failure analysis of cylindrical roller bearings has always been a hot research topic. Wang et al. deeply analyzed the ultrahigh cycle fatigue performance of GCr15 bearing steel [1]; Zou et al. analyzed the fracture failure of deep carburized bearing roller through experiments [2, 3]; Yan et al. summarized various factors affecting the fatigue life of rolling bearings [4]; Chen et al. put forward a theoretical formula for estimating crack growth on the basis of continuous tracking observation of contact fatigue spalling of bearing steel [5]; Lv et al. established a mathematical model to calculate the fatigue life of rolling bearings, simulated their experimental data by Monte Carlo method, and proposed a rolling bearing fatigue life prediction system [6]; Yang et al. organically combined the two processes of crack formation and crack propagation through damage mechanics and obtained a unified theoretical system through damage mechanics finite element analysis [7]. Zhang et al.

analyzed the contact stress and subsurface stress of cross roller rotary table bearing by theoretical method and finite element method [8]. Zhang et al. took the residual stress dispersion of the sequentially ground surface of bearing steel as the research object and tested the circumferential and axial residual stresses on the surface of the bearing race and the bearing raceway after the bearing race and raceway could not be precisely machined by X-ray diffraction method [9]. Zhu et al. studied the contact fatigue failure of cylindrical gears and explained the cause of surface pitting corrosion with excessive subsurface shear stress [10]. Yan et al. summarized various factors affecting the fatigue life of rolling bearings, especially analyzing the influence of maximum shear stress, maximum dynamic shear stress, von Mises stress, and octahedral shear stress on the fatigue life of rolling bearings [11]. Zhou analyzed various factors affecting contact fatigue wear of rolling bearings and pointed out that pitting and peeling of rolling surfaces are the manifestations of contact fatigue wear. Contact fatigue wear is caused by stress concentration, strain concentration, and plastic deformation of rolling surface [12]. Nguyen-Thanh [13] et al. proposed a new adaptive mesh-free configuration method for two-dimensional elastic and frictional contact analysis. Li et al. [14] proposed an isogeometric meshless configuration method for elastic fracture problems. Kruse and others [15] proposed an equivalent geometric formula for frictionless contact between deformable bodies based on the concept of the third medium. Huang and others [16] proposed a parallel simulation method that integrates the isogeometric meshless coupling method with the third medium method for contact problems.

At present, the domestic and foreign scholars' research on the failure of cylindrical roller fatigue bearings mainly focuses on the size of the stress, less on the stress distribution, especially on the subsurface stress. The fatigue fracture of cylindrical roller bearing is mainly the result of the formation and continuous expansion of cracks, and its failure is not only related to its surface material but also closely related to the size and distribution of working stress. Elastic composite cylindrical roller bearing is a new type of cylindrical roller bearing, as shown in Figure 1. Through the structural innovation design of cylindrical roller bearing, PTFE material is embedded in the deep hollow cylindrical roller to form an elastic composite cylindrical roller structure [17, 18], which increases the elasticity of the cylindrical roller, so as to increase the contact area between the roller and the inner and outer rings, reduce the contact stress between the roller and the raceway, improve the safe service life and bearing capacity of the cylindrical roller bearing, and also have obvious effect of vibration reduction and noise reduction. As a new type of cylindrical roller bearing, elastic composite cylindrical roller bearing [19–21] also has the problem of fatigue failure. Studying its subsurface stress is helpful to understand the rule of fatigue failure.

In this paper, three stages of the initiation, propagation, and falling off of the contact fatigue crack of the cylindrical roller bearing are analyzed theoretically. Subsurface stress is one of the factors of the contact fatigue failure. The distribution and magnitude of subsurface stress are calculated by analytical method. Based on the structural nonlinearity of elastic composite cylindrical roller bearing, its stress distribution and magnitude cannot be calculated by analytical method. The subsurface stress of ordinary cylindrical roller bearing and elastic composite cylindrical roller bearing with different fillings is calculated and analyzed by ANSYS software. The subsurface stress distribution of two types of cylindrical roller bearing and elastic composite cylindrical roller bearing with different fillings is compared. The distribution law of subsurface stress is obtained, which provides a basis for the study of fatigue failure mechanism of elastic composite cylindrical roller bearings.

2. Contact Fatigue Analysis of Cylindrical Roller Bearing

Many factors affect the contact fatigue failure of cylindrical roller bearings, including organization and defects, surface roughness/finish, contact stress, friction, lubrication state, residual stress, and bearing installation accuracy. Therefore, compared with general material fatigue failure, the influence factors of contact fatigue failure are more complex, which is also the reason why the contact fatigue failure mechanism is not completely clear at present. Because the effective area of cylindrical roller bearing stress will increase rapidly with the depth under the rolling surface, the high-pressure stress on the surface will not spread to the entire rolling element. Therefore, in rolling bearing design, the overall failure of rolling elements is usually not the main factor to be considered, but the failure of rolling surfaces is the focus of attention [22, 23]. The contact fatigue wear of cylindrical roller bearings is generally divided into three stages:

(1) *Fatigue crack initiation stage*: the location of fatigue crack source is often the place where rolling surface defects are serious and stress concentration occurs. The stress state here is three-way tensile stress, so fatigue cracks are easy to initiate here. In engineering, the fatigue crack initiation stage is defined as the crack depth of 0.05-0.08 mm

(2) *Fatigue crack growth stage*: under the action of external load, the fatigue crack extends to the center along the direction of 45° with the rolling contact surface. When the crack extends to a certain depth, it continues to expand in the direction parallel to the rolling contact surface under the action of subsurface stress

(3) *Fatigue peeling stage*: when the crack extends to a certain depth, the upper part of the crack end becomes a similar cantilever beam. Under the action of alternating bending stress, the root of the cantilever beam gradually tears and the section becomes smaller. Finally, it broke due to insufficient strength. The fractured cantilever beam becomes fragments and leaves the raceway surface, forming the so-called pitting and peeling phenomenon. According to the research of Littmann and Widner, the fatigue

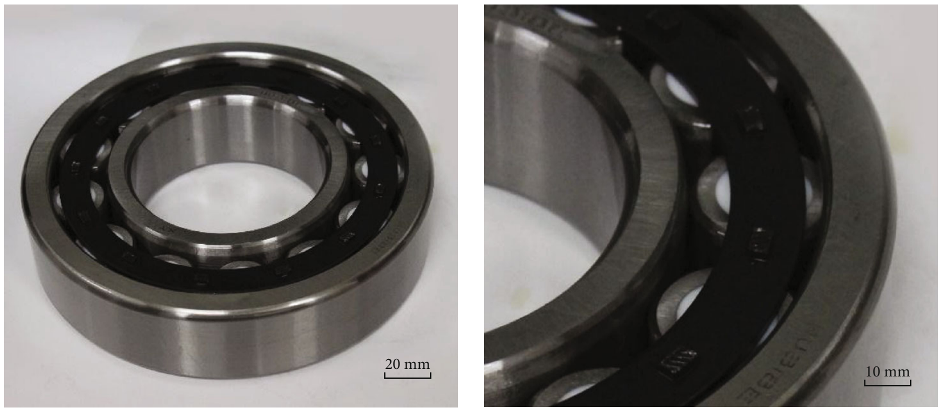

(a) Overall drawing

(b) Partial enlarged view

Figure 1: Physical drawing of elastic composite cylindrical roller bearing.

crack growth of cylindrical roller bearings depends on the magnitude of stress and the number of stress cycles. As shown in Figure 2, the relationship between stress and time varies according to the sine curve. The whole process of stress change from m to n is called a stress cycle. The time required to complete a stress cycle (T in the figure) is called a cycle. The maximum and minimum stresses in the cycle are represented by $\sigma_{\max}$ and $\sigma_{\min}$, respectively, and the ratio is called the cycle characteristic or stress ratio of the alternating stress. One-half of the algebraic sum of $\sigma_{\max}$ and $\sigma_{\min}$ is called the average stress, namely,

$$\sigma_{\mathrm{st}} = \frac{1}{2}\left(\sigma_{\max} + \sigma_{\min}\right). \quad (1)$$

One-half of the algebraic difference between $\sigma_{\max}$ and $\sigma_{\min}$ is called the stress amplitude, namely,

$$\sigma_{\mathrm{a}} = \frac{1}{2}\left(\sigma_{\max} \text{-} \sigma_{\min}\right). \quad (2)$$

2.1. Narrow Subsurface Stress. Lundberg and Palmgren put forward the theory of maximum dynamic shear stress. It is generally believed that the maximum dynamic shear stress parallel to the rolling direction under the contact surface is the main inducement to promote bearing fatigue failure, that is, the crack first occurs at the maximum dynamic shear stress and then expands to the surface, producing contact fatigue peeling [11].

Hertz contact theory is only applicable to the subsurface stress caused by the concentrated force acting vertically on the surface. The experimental data research shows that the bearing has spalling fatigue failure on the raceway surface, which originates from some weak points on the subsurface of the raceway. These points begin to appear initial cracks in the raceway under the alternating action of the rolling elements. The cracks gradually expand to the raceway surface under the alternating the subsurface stress and finally form

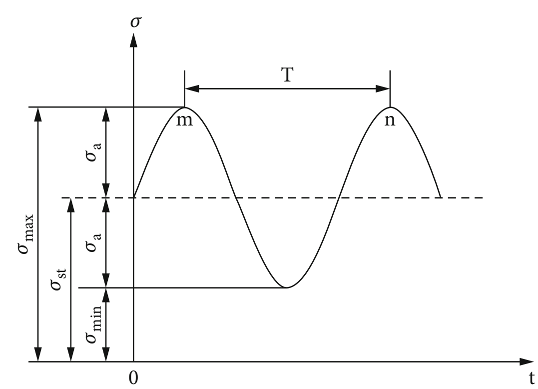

Figure 2: Alternating stress diagram.

surface peeling, Therefore, it is very important to study the magnitude of the subsurface stress of the raceway and its variation along the raceway depth when analyzing the fatigue life of the bearing. See Figure 3 for the theoretical basis of subsurface stress.

Considering only the stress generated by the concentrated force acting vertically on the surface, Jones used Thomas and Hoersch's method to give the formula for calculating the principal stresses S_x, S_y, and S_z at any depth along the z-axis under the contact surface. Since the surface stress on the z-axis is the maximum, the principal stress must also reach the maximum value on the surface, as shown in Figure 4.

$$S_x = M\left(\Omega_x + \nu\Omega_x'\right), \quad (3)$$

$$S_y = M\left(\Omega_y + \nu\Omega_y'\right), \quad (4)$$

$$S_z = -\frac{M}{2}\left(\frac{1}{\theta} - \theta\right), \quad (5)$$

$$\lambda = \frac{b\sum\rho}{(\kappa - (1/\kappa))\mathbf{E}\left(\left(\left(1 - \xi_1^2\right)/E_1\right) + \left(\left(1 - \xi_2^2\right)/E_2\right)\right)}, \quad (6)$$

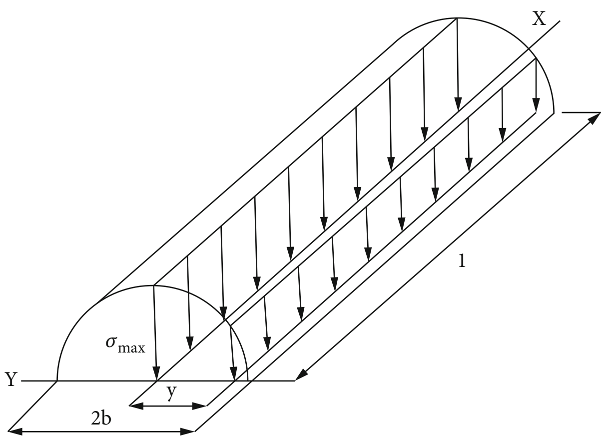

(a) Cyclic hertz stress of raceway contact surface

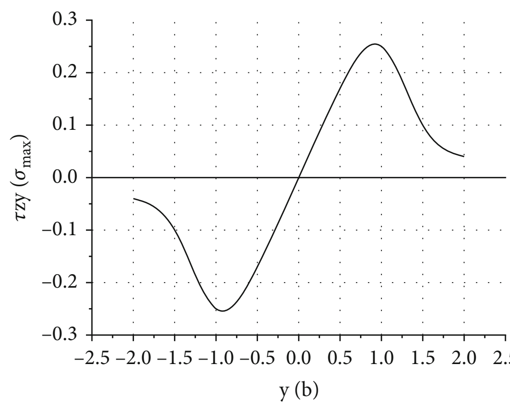

(b) Subsurface cyclic orthogonal shear stress

(c) Fatigue cracks on raceway

(d) Fatigue peeling of raceway

Figure 3: Fundamentals of subsurface stress theory.

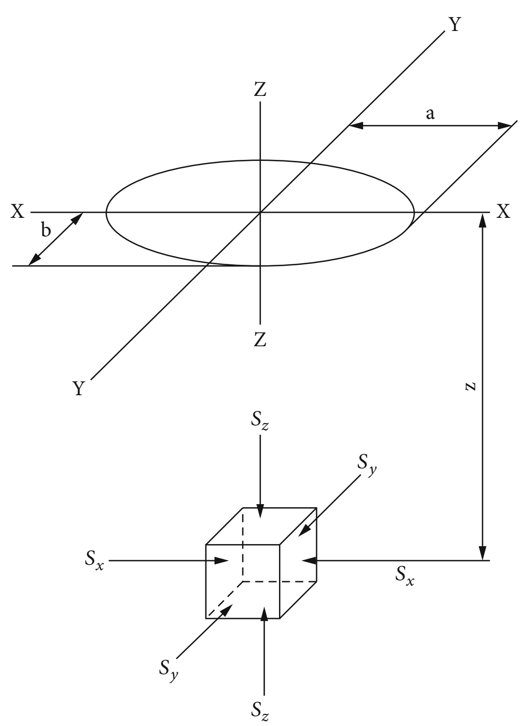

Figure 4: Principal stress on the z-axis below the surface.

$$\theta = \sqrt{\frac{\kappa^2 + \zeta^2}{1 + \zeta^2}}, \tag{7}$$

$$\zeta = \frac{z}{b}, \tag{8}$$

$$\kappa = \frac{a}{b}. \tag{9}$$

Here, a and b are the long and short half-axes of the projection ellipse of the contact area.

$$\Omega_x = -\frac{1}{2}(1-\theta) + \zeta[\mathbf{F}(\varphi) - \mathbf{E}(\varphi)], \tag{10}$$

$$\Omega'_x = 1 - \kappa^2\theta + \zeta\left[\kappa^2\mathbf{E}(\varphi) - \mathbf{F}(\varphi)\right], \tag{11}$$

$$\Omega_y = \frac{1}{2}\left(1 + \frac{1}{\theta}\right) - \kappa^2\theta + \zeta\left[\kappa^2\mathbf{E}(\varphi) - \mathbf{F}(\varphi)\right], \tag{12}$$

$$\Omega'_y = -1 + \theta + \zeta[\mathbf{F}(\varphi) - \mathbf{E}(\varphi)], \tag{13}$$

$$\mathbf{F}(\varphi) = \int_0^{\varphi}\left[1 - \left(1 - \frac{1}{\kappa^2}\right)\sin^2\varphi\right]^{-1/2}\mathbf{d}\varphi, \tag{14}$$

$$\mathbf{E}(\varphi) = \int_0^{\varphi}\left[1 - \left(1 - \frac{1}{\kappa^2}\right)\sin^2\varphi\right]^{1/2}\mathbf{d}\varphi. \tag{15}$$

After each maximum principal stress is determined, the maximum shear stress along the z-axis under the surface can be calculated. According to Mohr circle, the maximum shear stress is

$$\tau_{yz} = \frac{1}{2}\left(S_z - S_y\right), \tag{16}$$

$$b = \sqrt{\frac{4Q}{\pi l \sum \rho}\left(\frac{1-\upsilon_1^2}{E_1} + \frac{1-\upsilon_2^2}{E_2}\right)}. \tag{17}$$

As shown in Figure 4, the maximum shear stress occurs at different depths z under the surface. For simple point contact, this depth is $0.467b$, while for line contact, it is $0.786b$.

2.2. Generalized Subsurface Stress. After Lundberg and Palmgren, Ioannides, Harris, Zeretsky, Cheng Wangquan, and Cheng Herbert successively used the maximum von Mises stress under the surface, the maximum static shear stress, and the maximum octahedral shear stress as the inducing factors for the occurrence and propagation of contact fatigue cracks. Subsurface stress is defined by shear stress in a narrow sense as the stress that induces the occurrence and propagation of contact fatigue cracks under the surface in a broad sense. The research on contact fatigue crack growth of cylindrical roller bearing with contact stress should be carried out from the generalized subsurface stress. Under the condition of good lubrication, the friction between the rolling element and the raceway has a limited effect on the stress distribution. Ignoring the influence of friction factors can usually get better results in most applications.

3. Finite Element Model and Analysis

Due to the structural nonlinearity of elastic composite cylindrical roller bearings, the theoretical analysis can only be carried out by means of numerical analysis instead of analytical method. In order to study the distribution and magnitude of subsurface stress of cylindrical roller bearing and elastic composite cylindrical roller bearing [10] in the working process, the corresponding finite element model is established in the ANSYS software.

3.1. Finite Element Modeling. Cylindrical roller bearing is a highly symmetrical structure, and its symmetry can be fully used to simplify the model in finite element modeling to reduce the amount of calculation. The shape structure of the elastic composite cylindrical roller bearing is the same as that of the ordinary cylindrical roller bearing. The main difference in modeling is the rolling element. The elastic composite cylindrical roller is a noncontinuum composed of two materials. Through preliminary analysis and comparison, it is reasonable to use 1/2 cylindrical roller and part of bearing inner race to establish finite element analysis model, as shown in Figure 5.

3.2. Grid Division. Through the analysis of cylindrical roller bearings, the materials of inner and outer rings, hollow rollers, and solid rollers are GCr15 bearing steel, with an elastic modulus of 206 GPa and Poisson's ratio of 0.3. The elastic modulus of PTFE embedded in the elastic composite cylindrical roller is 280 MPa, and Poisson's ratio is 0.4. Considering the continuity of analysis, SOLID186 unit is selected, and CONTA174-TARGE170 face to face contact analysis method is selected as the contact model. In order to improve the accuracy of nonlinear analysis and calculation, the contact parts were refined. The accuracy and efficiency of finite element analysis are closely related to element density and element geometry. Too dense grid may result in too long calculation time, while too sparse grid cannot accurately

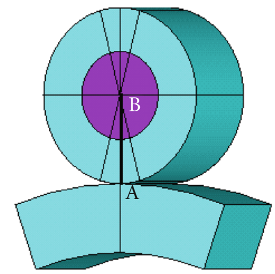

Figure 5: Finite element modeling.

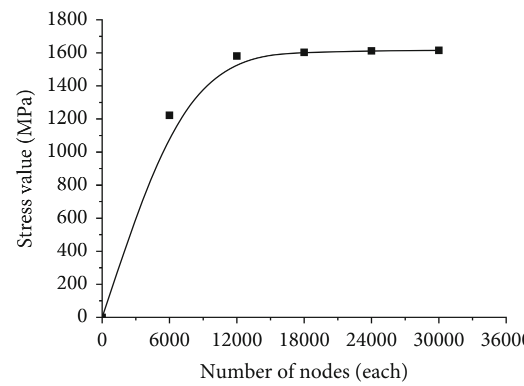

Figure 6: Relationship between stress value and number of model nodes.

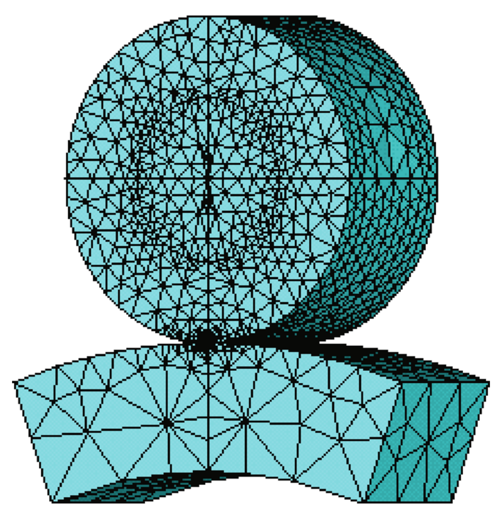

Figure 7: Mesh generation model.

Table 1: Constraints.

Constraint position	Constraint status					
	U1	U2	U3	UR1	UR2	UR3
Lower bottom of the inner race	–	√	–	–	–	–
Inner ring side	–	–	√	–	–	–
Rolling body side	–	–	√	–	–	–
The middle section of the rolling body	√	–	–	–	–	–

Table 2: NU318E bearing external dimension parameter.

Bearing inside diameter d (mm)	90	Rolling element diameter D_1 (mm)	28
Bearing outside diameter D (mm)	190	Rolling element length L (mm)	30
Bearing width B (mm)	43	Rolling element number Z (each)	13

Table 3: Comparison between theoretical calculation value and simulation calculation value.

Theoretical calculation value of maximum shear stress (MPa)	Simulation calculation value of maximum shear stress (MPa)	Relative error percentage (%)	Theoretical calculation value of maximum shear stress depth (mm)	Simulation calculation value of maximum shear stress depth (mm)	Relative error percentage (%)
24.67	25.89	4.7	0.685	0.713	3.9

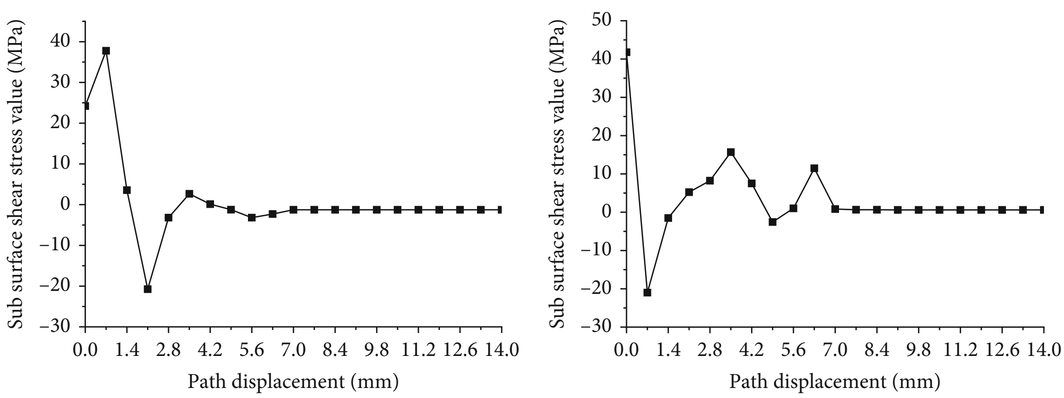

(a) Cylindrical roller bearing (b) Elastic composite cylindrical roller bearing

Figure 8: Subsurface shear stress path diagram.

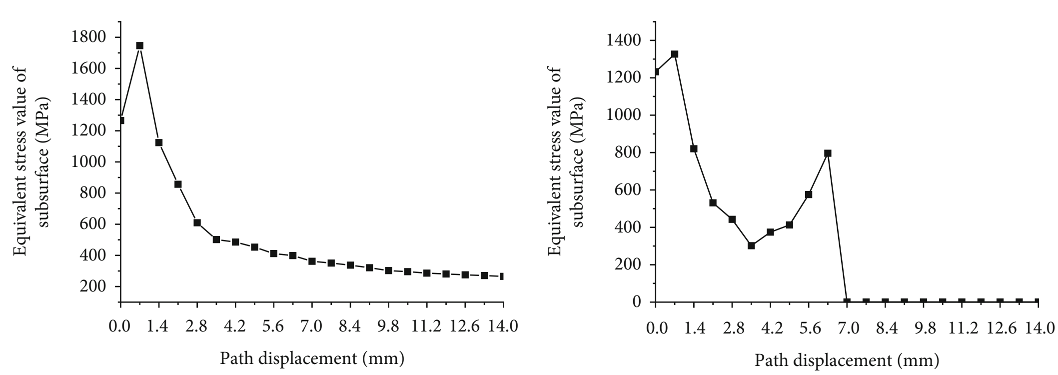

(a) Cylindrical roller bearing (b) Elastic composite cylindrical roller bearing

Figure 9: Equivalent stress path diagram of subsurface.

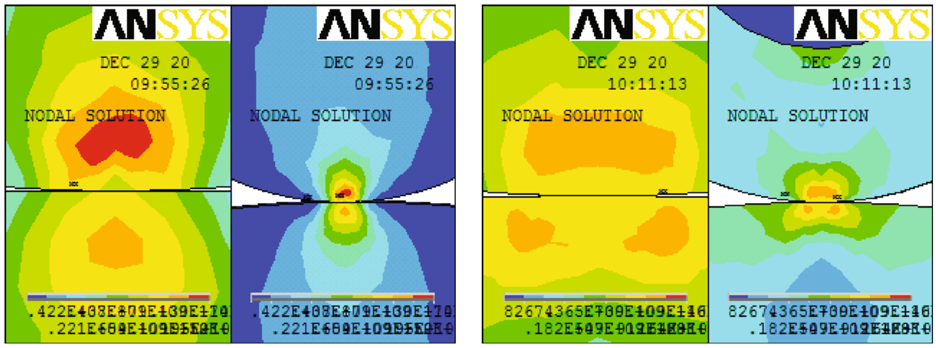

(a) Cylindrical roller bearing

(b) Elastic composite cylindrical roller bearing

FIGURE 10: Equivalent stress cloud maps of two types of cylindrical roller bearings on the subsurface.

describe the spatial changes of field variables. Therefore, the mesh is subdivided appropriately at the contact part between the solid cylindrical roller and the inner and outer rings to improve the calculation accuracy. The other overall parts can be roughly divided to save calculation time when the accuracy is not affected. For whether the overall division density setting is reasonable, the influence of different densities on the calculation results obtained through a large number of finite element analysis is shown in Figure 6. It can be seen from the figure that the model grid division of 11605 nodes and 55322 elements is reasonable, and the grid division model is shown in Figure 7.

3.3. Constraints and Loads. According to the working characteristics and force characteristics of cylindrical roller bearings, the definition and constraints of the finite element model are as follows: impose Y direction constraints on the lower bottom of the inner race, impose Z direction constraints on the inner race and the side of the rolling body, and impose X direction symmetric constraints on the middle section of the rolling body. See Table 1 for constraints. The loading of rolling element is simulated by defining function loading mode.

3.4. Calculation Strategy. The external dimensions of the two cylindrical roller bearings are the same, but the internal structures are different. In order to compare the subsurface stress of the two cylindrical roller bearings scientifically and effectively, it is necessary to establish a reasonable finite element calculation strategy. When the overall dimensions are fixed, the optimal filling degree of the elastic composite cylindrical roller bearing is related to the external load. Generally, the optimal filling degree is 55% for heavy load and 65% for light load. In order to study the subsurface stress of different cylindrical roller bearings and the influence of elastic composite cylindrical roller bearings with different filling degrees on the subsurface, longitudinal and transverse comparative analysis and calculation are adopted, as shown below.

(1) *Longitudinal calculation*: the maximum orthogonal tangential stress and its distribution of cylindrical roller bearing are calculated by analytical method, and the error analysis is carried out by comparing the results calculated by analytical method and finite element method. The size and distribution of the subsurface stress (the maximum orthogonal shear stress and the maximum von Mises stress) of two kinds of cylindrical roller bearings are analyzed through the simulation theoretical calculation of

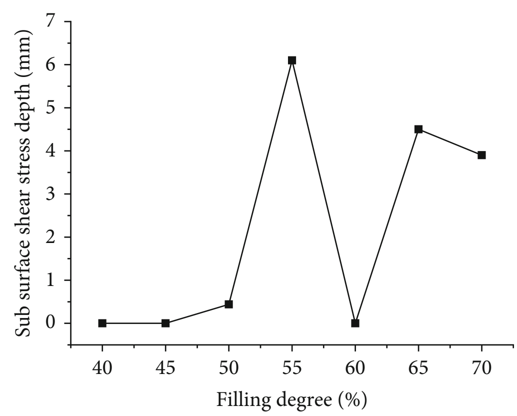

FIGURE 11: Relationship between the depth of secondary surface shear stress and filling degree.

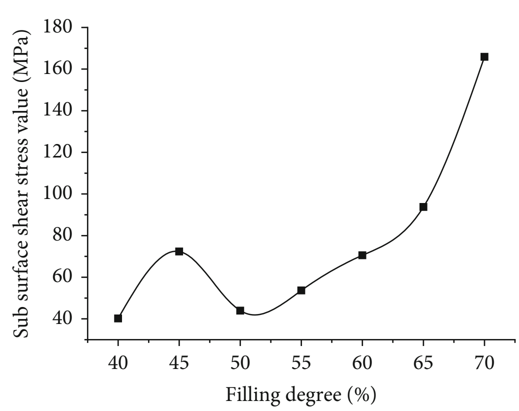

FIGURE 12: Relationship between subsurface shear stress and filling degree.

Table 4: Analysis of the results of subsurface shear stress.

Filling degree interval of elastic composite cylindrical roller	Subsurface equivalent stress		Reason
	Depth change trend	Size change trend	
40%-55%	Rise	Raise first and then lower	With the increase of filling degree, the rigidity of elastic composite cylindrical roller decreases, the contact half width increases, the depth of subsurface shear stress also increases, and the shear stress varies irregularly.
55%-60%	Reduce	Rise	With the increase of the filling degree, the mechanical properties of the bearing materials show a nonmonotonic change. The filling degree of the elastic composite cylindrical roller reaches the peak at 55% of the subsurface shear stress depth, the stress value is not large, and the stress continues to increase.
60%-70%	Rise	Rise	With the increase of filling degree of elastic composite cylindrical roller, the stress of bearing material under load has exceeded its limit, so the subsurface shear stress presents a monotonous upward trend.

cylindrical roller bearings with the same overall dimensions and elastic composite cylindrical roller bearings with 50% filling degree

(2) *Horizontal calculation*: through numerical calculation and analysis of elastic composite cylindrical roller bearing with the same overall dimension and different material filling degrees, the influence of different material filling degrees on the magnitude and distribution of the subsurface stress (maximum orthogonal shear stress and maximum von Mises stress) of elastic composite cylindrical roller bearing is studied

4. Calculation Example

Taking NU318E cylindrical roller bearing as an example, the boundary dimensions of elastic composite cylindrical roller bearing NU318E are selected for analysis and calculation. The external dimension parameters of NU318E bearing are shown in Table 2.

4.1. Comparison between Analytical Method and Finite Element Method. Under the same conditions, the maximum shear stress and depth of the secondary surface of NU318E cylindrical roller bearing are analyzed and calculated by the analytical method and the finite element method. See Table 3 for the comparative analysis of the theoretical calculation value and the finite element calculation value calculated according to Formulas (16) and (17). In the table, relative error = $[(\text{simulation calculated value} - \text{theoretical calculated value})/\text{simulation calculated value}] \times 100\%$.

It can be seen from Table 3 that under the same conditions, the errors of the calculated values obtained by the two calculation methods are within 10%, which indicates that the finite element modeling and calculation of solid cylindrical rolling bodies are scientific and accurate. Because the contact between the elastic composite cylindrical roller and the inner and outer rings does not conform to the basic assumptions of Hertz contact theory, the relevant parameters cannot be calculated with Formulas (16) and (17), while the elastic composite cylindrical roller and the solid cylindrical roller only have differences in the internal structure of the roller, and the contact pairs formed by the inner and outer rings of the two are similar. According to the above

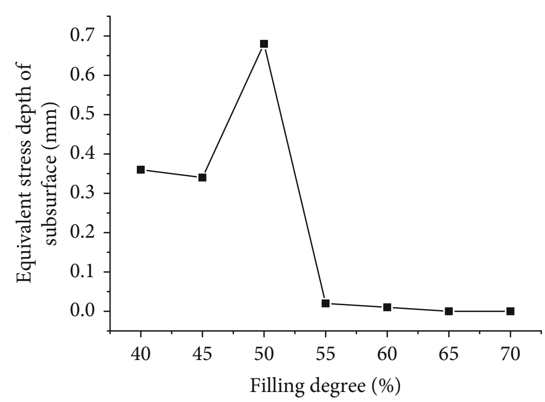

Figure 13: Relationship between equivalent stress depth of subsurface and filling degree.

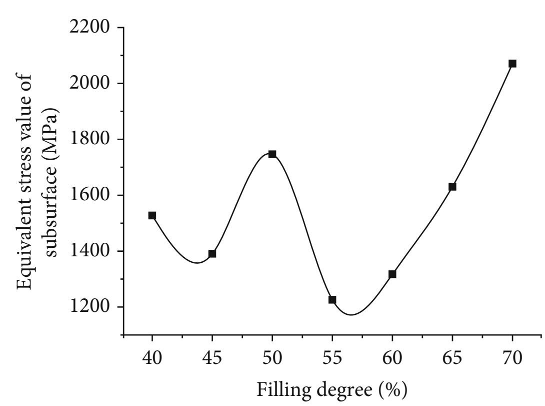

Figure 14: Relationship between equivalent stress of subsurface and filling degree.

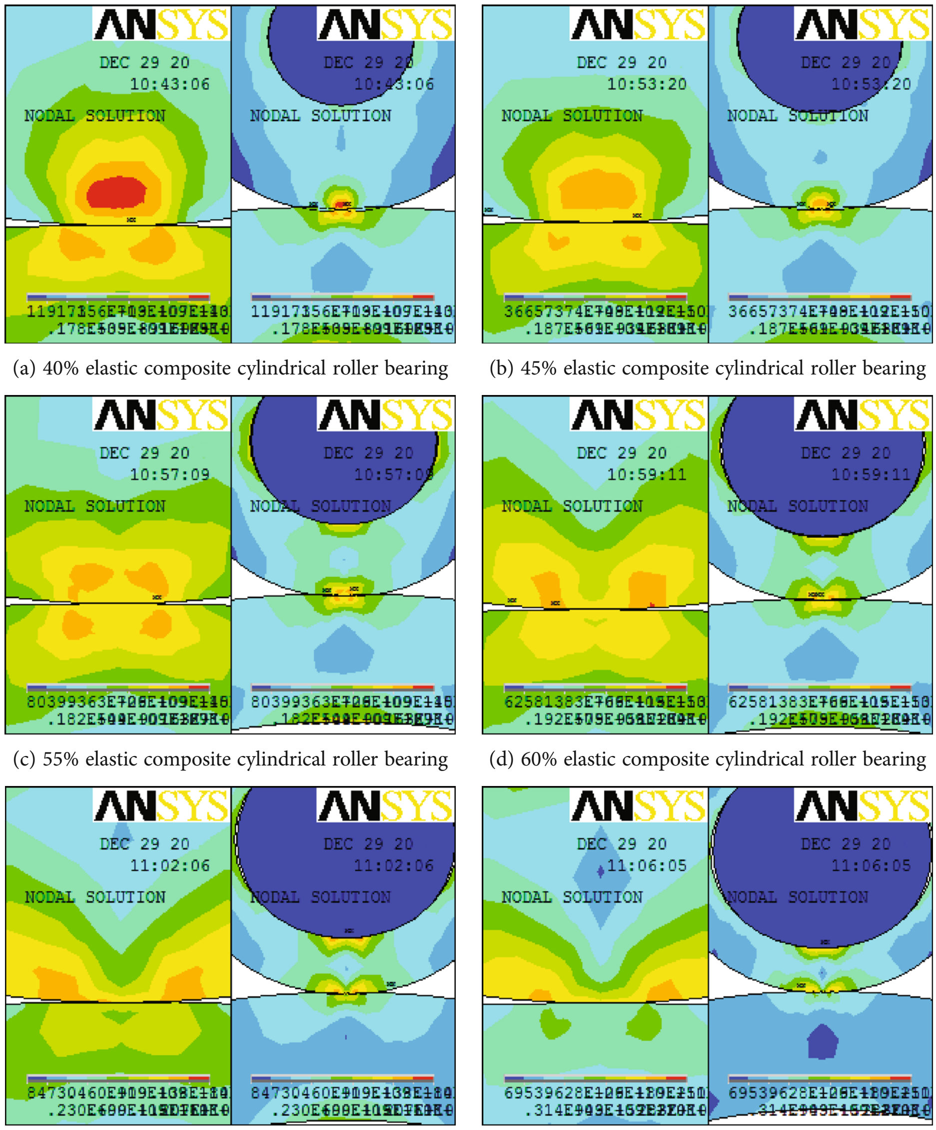

(a) 40% elastic composite cylindrical roller bearing

(b) 45% elastic composite cylindrical roller bearing

(c) 55% elastic composite cylindrical roller bearing

(d) 60% elastic composite cylindrical roller bearing

(e) 65% elastic composite cylindrical roller bearing

(f) 70% elastic composite cylindrical roller bearing

Figure 15: Subsurface equivalent stress cloud map of elastic composite cylindrical roller bearings with different filling degrees.

comparative analysis, the finite element method can be used to simulate the elastic composite cylindrical roller bearing.

4.2. Comparison of Subsurface Stress Results of Two Types of Cylindrical Roller Bearings. Numerical simulation of Nu318e cylindrical roller bearing and Nu318e elastic compound cylindrical roller bearing is carried out. The subsurface stress calculation results of two kinds of cylindrical roller bearings are shown in Figures 8 and 9. The stress path diagram uses the AB line (see Figure 5) as the path to count the stress of the path. Obviously, the 0 point of the abscissa of the path diagram represents the surface of the rolling body. When the abscissa value is greater than 0, its physical meaning is that it is below the surface, and the greater the value is, the farther it is from the surface.

Figure 8 shows the subsurface shear stress path diagram of two kinds of cylindrical roller bearings. According to the figure, the maximum subsurface shear stress of cylindrical roller bearing is 37.78 MPa near 0.69 mm below the surface, while the maximum shear stress of elastic composite cylindrical roller bearing is 43.951 MPa on the surface of the rolling body. The maximum shear stress distribution of the two types of cylindrical roller bearing is not consistent, and the maximum shear stress does not exist on the subsurface of elastic composite cylindrical roller bearing.

Figure 9 shows the equivalent stress path diagram of the secondary surface of two kinds of cylindrical roller bearings, and Figure 10 shows the equivalent stress cloud diagram of the corresponding secondary surface. According to Figure 9, the maximum equivalent stress on the secondary surface of cylindrical roller bearing at 0.7 mm below the surface is 1746.525 MPa, while the maximum equivalent stress on the secondary surface of elastic composite cylindrical roller bearing at 0.44 mm below the surface is 1326.6 MPa. The subsurface stress of elastic composite cylindrical roller bearings is 31.65% smaller than that of ordinary cylindrical roller

Table 5: Analysis of the results of subsurface equivalent stress.

Filling degree interval of elastic composite cylindrical roller	Variation trend of equivalent stress		Reason
	Depth change trend	Size change trend	
40%-45%	Reduce	Reduce	With the increase of filling degree, the rigidity of elastic composite cylindrical roller decreases, the contact half width increases, and the stress values decrease.
45%-55%	Raise first and then lower	Raise first and then lower	The mechanical properties of the elastic composite cylindrical roller vary nonmonotonously from 45% to 55% of the filling degree, thus forming an inflexion point, so there is a peak value of the equivalent stress region on the subsurface.
55%-70%	Reduce	Rise	With the increase of filling degree of elastic composite cylindrical roller, the stress of bearing material under load has exceeded its limit, so the equivalent stress of subsurface presents a monotonous upward trend. The maximum equivalent stress of filling degree in this range is basically on the surface of the elastic composite cylindrical roller, mainly due to the excessive filling and the increased flexibility.

bearings, and the distribution of the maximum subsurface stress of elastic composite cylindrical roller bearings is shallower than that of cylindrical roller bearings.

To sum up, because the elastic composite cylindrical roller is more flexible than the cylindrical roller, the subsurface stress distribution of the roller is different, and the maximum subsurface stress distribution of the elastic composite cylindrical roller bearing is shallower than that of the cylindrical roller bearing.

4.3. Effect of Material Filling Degree on Subsurface Stress Distribution. Through finite element analysis of elastic composite cylindrical roller bearings with different filling degrees, the magnitude and distribution of subsurface shear stress and subsurface equivalent stress of elastic composite cylindrical roller are mainly analyzed. The results are as follows.

4.3.1. Analysis of Subsurface Shear Stress. Figures 11 and 12, respectively, show the relationship between the depth and size of the subsurface shear stress and the degree of filling of the elastic composite cylindrical roller bearing. According to the figure, the relationship between the depth and size of the subsurface shear stress and the filling degree does not continuously show regular changes. The specific analysis is shown in Table 4.

4.3.2. Subsurface Equivalent Stress Analysis. Figures 13 and 14, respectively, show the relationship between the depth and size of the equivalent stress on the subsurface of the elastic composite cylindrical roller bearing and the filling degree, and Figure 15 shows the cloud diagram of the equivalent stress on the subsurface of the elastic composite cylindrical roller bearing under different filling degrees. According to the figure, the relationship between the depth and size of the equivalent stress on the subsurface and filling degree did not show a continuous regular change. The specific analysis is shown in Table 5.

According to a large number of basic research and analysis, the comprehensive performance indicators of elastic composite cylindrical roller bearings, such as contact stress, von Mises stress, bending stress, and deformation, are in the optimal range of 55% to 65% filling degree. According to the analysis of the results in Table 4, for elastic composite cylindrical roller bearings with a filling degree of 55%-65%, the subsurface shear stress value is maintained at a low level, and the depth of the shear stress is minimal, which is basically distributed on the surface of the rolling element. According to the analysis of the results in Table 5, the elastic composite cylindrical roller bearing with a filling degree of 55%-65% has the smallest equivalent stress value on the subsurface, and its equivalent force depth is also the smallest, which is basically distributed on the surface of the rolling body.

5. Conclusion

(1) The contact fatigue of cylindrical roller bearing is analyzed, and the subsurface stress is one of the failure factors of contact fatigue. Subsurface stress includes shear stress and equivalent stress

(2) The shear stress on the subsurface of cylindrical roller bearing is calculated by analytical method and finite element method. The comparison results show that the calculation of finite element method is scientific and accurate

(3) The subsurface stresses of cylindrical roller bearings and elastic composite cylindrical roller bearings are analyzed by finite element method. The results show that the magnitude and distribution of the subsurface stresses of the two types of cylindrical roller bearings are different. The subsurface stress of elastic composite cylindrical roller bearings is 31.65% smaller than that of ordinary cylindrical roller bearings, and the distribution of the maximum subsurface stress of elastic composite cylindrical roller

bearings is shallower than that of cylindrical roller bearings. In summary, elastic composite cylindrical roller bearings have significant advantages over cylindrical roller bearings in terms of subsurface stress and have stronger resistance to contact fatigue damage

(4) Through the analysis of elastic composite cylindrical roller bearings with different filling degrees, the magnitude and distribution of subsurface stress are preliminarily obtained. For elastic composite cylindrical roller bearings with filling degrees of 55% to 65%, the subsurface shear stress and equivalent stress values are maintained at a relatively low level, and the depth of the maximum stress is minimal, which is basically distributed on the surface of the rolling body

Data Availability

The data are in the article.

Conflicts of Interest

The authors declare that they have no conflicts of interest.

Acknowledgments

The authors are grateful to the National Natural Science Foundation of China (51175168) and Hunan Province Natural Science Foundation (2021JJ60069 and 2021JJ50054) and Excellent Youth Project of Hunan Provincial Department of Education (No. 21B0897) for their support.

References

[1] Q. Y. Wang, H. Y. Zhang, M. R. Sriraman, and S. X. Li, "Very long life fatigue behavior of bearing steel AISI 52100," *Key Engineering Materials*, vol. 297-300, pp. 1846–1851, 2005.

[2] Z. Yong, D. Wei-Juan, L. Xue-Xiang, and C. Guo-Dong, "Failure analysis of bearing roller after deep carburizing and quenching," *Heat Treatment of Metals*, vol. 36, no. 9, pp. 91–94, 2011.

[3] Z. Longjiang, Z. Quan, and G. Lusi, "Fracture failure analysis of G20Cr2Ni4A steel bearing roller," *Heat Treatment of Metals*, vol. 10, pp. 101–103, 2013.

[4] Y. Jian-Hui, L. I. Xing-Lin, J. Wan-li, Z. Yan-Liao, and W. Jiu-Gen, "Progress of fatigue life theory of bearings," *Bearing*, vol. 11, pp. 38–44, 2005.

[5] C. Long-Qing and C. Qing, "Tracking observation on subsurface cracking in GCr15 bearing steel under rolling contact fatigue," *Acta Metallurgica Sinica*, vol. 27, no. 5, pp. 61–65, 1991.

[6] L. Hua-Qiang, W. Li-Qin, G. Le, and L. Wen-Zhong, "The simulating technique for fatigue lives of rolling element bearing," *Mechanical Research&Application*, vol. 18, no. 5, pp. 42–44, 2005.

[7] Y. Ji-Yun, Z. Xing, and Z. Min, "Numerical method for crack extension analysis based on fatigue crack formation curve," *Chinese Journal of Mechanical Engineering*, vol. 40, no. 7, pp. 55–62, 2004.

[8] Z. Xue, Z. Gang, Z. Kai-Feng, L. Ming-Yan, and Z. Jian, "FEA of cross—roller slewing bearings," *Bearing*, vol. 4, pp. 1–4, 2012.

[9] Z. Xue-Ping, W. He-Ping, L. Guang-Hui, and G. Er-Wei, "Experimental study on surface residual stress scatter of bearing steel produced by sequential grinding processes," *Journal of Mechanical Engineering*, vol. 46, no. 15, pp. 89–94, 2010.

[10] Z. You-Li, W. Yan-Li, B. Fei-Long, H. Shuai, and Y. Hong-Jun, "Re-examining the origins of contact fatigue failure of involute cylindrical spur gears," *Tribology*, vol. 34, no. 6, pp. 722–728, 2014.

[11] Y. Jian-Hui and W. Jiu-Gen, "Influence factors on fatigue life of rolling bearing," *Bearing*, vol. 6, pp. 21–25, 2003.

[12] Z. Hai-Shan, "Influence of surface state on contact fatigue wear of rolling bearing," *China Surface Engineering*, vol. 2, pp. 35–38, 1994.

[13] N. Nguyen-Thanh, W. Li, J. Huang, N. Srikanth, and K. Zhou, "An adaptive isogeometric analysis meshfree collocation method for elasticity and frictional contact problems," *International Journal for Numerical Methods in Engineering*, vol. 120, no. 2, pp. 209–230, 2019.

[14] W. Li, N. Nguyen-Thanh, and K. Zhou, "An isogeometric-meshfree collocation approach for two-dimensional elastic fracture problems with contact loading," *Engineering Fracture Mechanics*, vol. 223, article 106779, 2020.

[15] R. Kruse, N. Nguyen-Thanh, P. WriggersDe, and L. Lorenzis, "Isogeometric frictionless contact analysis with the third medium method," *Computational Mechanics*, vol. 62, no. 5, pp. 1009–1021, 2018.

[16] J. Huang, N. Nguyen-Thanh, and K. Zhou, "An isogeometric-meshfree coupling approach for contact problems by using the third medium method," *International Journal of Mechanical Sciences*, vol. 148, pp. 327–336, 2018.

[17] Y. Qishui, Y. Wen, Y. Jianghong, and Z. Ran, "Research on structure design of elastic composite cylindrical roller bearing," *China Mechanical Engineering*, vol. 23, no. 24, pp. 2899–2902, 2012.

[18] Y. Qishui, Y. Wen, Y. Dejie, and Y. Jianghong, "Bending stress of rolling element in elastic composite cylindrical roller bearing," *Journal of Central South University*, vol. 20, no. 12, pp. 3437–3444, 2013.

[19] Y. Qishui, C. Qianxu, Y. Jianghong, and Y. Wen, "Structures dynamic property analysis of elastic composite cylindrical rolling element," *International Journal of Rotating Machinery*, vol. 2021, Article ID 4244659, 8 pages, 2021.

[20] Y. Jianghong, Y. Wen, L. Chao, and Y. Qishui, "Machining technology for elastic composite cylindrical rollers," *China Mechanical Engineering*, vol. 26, no. 12, pp. 1616–1621, 2015.

[21] Y. Jianghong, X. Lei, Y. Wen, L. Chao, D. Yaoyao, and Y. Qishui, "Modal and harmonic response analysis of a rolling bearing coupled by rigid and flexible materials," *Materials Express*, vol. 9, no. 9, pp. 1017–1024, 2019.

[22] T. A. Harris, "Roller bearing analysis: original version 5, volume 1, basic concepts of bearing technology," China Machine Press, Beijing, 2009.

[23] T. A. Harris, "Roller bearing analysis: original version 5, volume 2, advanced concept of bearing technology," China Machine Press, Beijing, 2009.